HHS Public Access

Author manuscript

Neuropharmacology. Author manuscript; available in PMC 2021 February 14.

Published in final edited form as:

Neuropharmacology. 2020 January 01; 162: 107827. doi:10.1016/j.neuropharm.2019.107827.

Affinity-matured 'aquaporumab' anti-aquaporin-4 antibody for therapy of seropositive neuromyelitis optica spectrum disorders

Tianjiao Duan[1,2], **Lukmanee Tradtrantip**[1], **Puay-Wah Phuan**[1], **Jeffrey L. Bennett**[3], **Alan S. Verkman**[1]

[1]Departments of Medicine and Physiology, University of California, San Francisco, CA 94143, U.S.A.

[2]Department of Neurology, Second Xiangya Hospital of Central South University, Changsha, 410011, Hunan, China

[3]Departments of Neurology and Ophthalmology, Programs in Neuroscience and Immunology, University of Colorado Anschutz Medical Campus, Denver, CO 80045, U.S.A.

Abstract

Pathogenesis in seropositive neuromyelitis optica spectrum disorders (herein called NMO) involves binding of IgG1 autoantibodies to aquaporin-4 (AQP4) on astrocytes in the central nervous system, which initiates complement and cellular injury. We previously developed an antibody blocking approach for potential therapy of NMO in which an engineered, monoclonal, anti-AQP4 antibody lacking cytotoxicity effector functions (called aquaporumab) blocked binding of NMO autoantibodies to astrocyte AQP4 (Tradtrantip et al. Ann. Neurol. 71, 314–322, 2012). Here, a high-affinity aquaporumab, which was generated by affinity maturation using saturation mutagenesis, was shown to block cellular injury caused by NMO patient sera. Anti-AQP4 antibody rAb-53, a fully human antibody with effector function neutralizing Fc mutations L234A/L235A and affinity-enhancing Fab mutations Y50R/S56R, called AQmab^{AM}, bound to AQP4 in cell cultures with K_d ~ 18 ng/ml (~ 0.12 nM), ~8-fold greater affinity than the original antibody. AQmab^{AM}, but without L234A/L235A Fc mutations, produced complement-dependent cytotoxicity (CDC) with EC_{50} ~ 82 ng/ml. AQmab^{AM} prevented CDC produced by sera from eight NMO patients with IC_{50} ranging from 40–80 ng/ml, and similarly prevented antibody-dependent cellular cytotoxicity (ADCC). Mechanistic studies demonstrated that AQmab^{AM} blocked binding of serum NMO autoantibodies to AQP4. AQmab^{AM} offers a targeted, non-immunosuppressive approach for therapy of seropositive NMO. Autoantibody blocking may be a useful therapeutic strategy for other autoimmune diseases as well.

Correspondence to: Alan S. Verkman, M.D., Ph.D., 1246 Health Sciences East Tower, 513 Parnassus Ave, San Francisco, CA 94143-0521, U.S.A., Alan.Verkman@ucsf.edu, Phone: (415) 476-8530, Fax: (415) 665-3847.

Disclosure/conflict of interest

JLB and ASV are named inventors on a patent application on aquaporumab antibodies for treatment NMO, whose rights are owned by the University of Colorado and the University of California. The other authors have no conflicts of interest.

Keywords

NMOSD; autoimmunity; blocking antibody; AQP4; astrocyte

1. Introduction

Neuromyelitis optica spectrum disorder (NMOSD) is an inflammatory disease of the central nervous system (CNS) that is associated with demyelination and neurological deficits in optic nerve, spinal cord and brainstem. Most NMOSD patients are seropositive for IgG autoantibodies directed against extracellular epitopes of aquaporin-4 (AQP4) (Lennon et al., 2005), a water channel expressed on astrocytes throughout the CNS and in skeletal muscle and some epithelial cells outside of the CNS (Papadopoulos and Verkman, 2012; Mader and Brimberg, 2019). There is abundant evidence from human pathological specimens and experimental animal models that the anti-AQP4 autoantibodies (called AQP4-IgG) are pathogenic in seropositive NMOSD (herein called NMO) (Misu et al., 2007; Graber et al., 2008; Lucchinetti et al., 2002; Papadopoulos and Verkman, 2012; Tradtrantip et al., 2017; Weinshenker and Wingerchuk, 2017). AQP4-IgG binding to AQP4 on astrocytes causes injury to astrocytes and surrounding bystander cells by complement-dependent cytotoxicity (CDC) and antibody-dependent cellular cytotoxicity (ADCC) mechanisms, producing inflammation and blood-brain barrier disruption that leads to oligodendrocyte injury and demyelination. Current NMO therapies include immunosuppression, B cell depletion and plasma exchange (Jarius et al., 2014; Papadopoulos et al., 2014), with newer therapies, including complement C5 inhibition, IL-6 receptor inhibition, and CD19 inhibition, in clinical trials (Bruscolini et al., 2018; Collongues et al., 2019).

As binding of pathogenic AQP4-IgG autoantibodies to plasma membrane AQP4 is the primary initiating event in NMO pathogenesis, we reasoned that blocking this interaction could have therapeutic benefit in NMO. High-throughput screening identified small-molecule blockers of AQP4-IgG binding to AQP4 (Tradtrantip et al., 2012a), though their potency and CNS penetration were low. We subsequently developed an alternative and highly specific blocking approach involving an engineered, monoclonal anti-AQP4 antibody to block binding of pathogenic AQP4-IgG to AQP4 (Tradtrantip et al., 2012b). The blocking antibody, called ‘aquaporumab’, was generated from rAb-53, a high-affinity human monoclonal AQP4-IgG derived from sequence analysis of plasma cells in cerebrospinal fluid of an NMO patient (Bennett et al., 2009), in which Fc mutations L234A/L235A were introduced to neutralize antibody CDC and ADCC effector functions. The resultant aquaporumab, at sufficiently high concentration, blocked CDC and ADCC caused by AQP4 in cell cultures and brain slices, and reduced pathology in a mouse model of NMO.

Here, to advance the aquaporumab blocking antibody approach, an affinity-matured antibody was generated and characterized for AQP4 binding, competitive displacement of AQP4-IgG, and prevention of complement- and cell-mediated cytotoxicity produced by NMO patient sera in AQP4-expressing cell cultures.

2. Material and Methods

2.1 Antibodies and affinity maturation

Recombinant monoclonal NMO antibody (rAb-53) of IgG1 subtype was generated from sequence analysis of clonally expanded plasma cells in cerebrospinal fluid, as described and characterized previously (Bennett et al., 2009; Crane et al., 2011). Affinity maturation was done by saturation mutagenesis in which each amino acid in the complementary determining regions (CDRs) of rAb-53 was individually mutated to 15 other amino acids, and resultant IgG antibodies screened in a cell-based AQP4 ELISA binding assay (BioAtla, San Diego, CA); antibodies with single mutations having >3-fold enhanced AQP4 binding affinity were re-generated with double mutation combinations and tested. L234A/L235A point mutations were introduced into the IgG1 Fc sequence to generate antibodies deficient in CDC and ADCC effector functions. The affinity-matured aquaporumab with highest AQP4 binding affinity, Y50R/S56R, is referred to as $AQmab^{AM}$.

2.2 Human NMO sera

Sera from confirmed AQP4-IgG seropositive NMO patients, and non-NMO control sera, were obtained from the Circles Repository of the Guthy-Jackson Charitable Foundation. Seropositive serum samples were randomly selected without reference to clinical information.

2.3 Cell culture

Chinese hamster ovary (CHO) cells stably expressing M23-AQP4 (CHO-AQP4 cells) were used, as described (Crane et al., 2011; Phuan et al., 2013). CHO cells were cultured at 37 °C in 5% CO_2 95% air in F-12 Ham's Nutrient Mixture medium supplemented with 10% fetal bovine serum, 200 μg/ml geneticin, 100 U/ml penicillin and 100 μg/ml streptomycin. Human natural killer cells (NK cells) expressing the high-affinity 176V variant of the Fcγ receptor IIIA were obtained from Fox Chase Cancer Center (Philadelphia, PA). NK cells were cultured in suspension in α-MEM (Sigma-Aldrich, St. Louis, MO) containing 0.1 mM 2-mercaptoethanol, 2 mM L-glutamine, 0.2 mM myoinositol, 10% FBS, 10% horse serum, 2.5 μM folic acid, non-essential amino acids, 1 mM Na pyruvate, 100 U/ml penicillin, 100 μg/ml streptomycin, and 100 IU/ml of human recombinant interleukin-2 (GenScript, Piscataway, NJ). Primary astrocyte cultures were generated from cerebral cortex of neonatal rats as described (Duan et al., 2018).

2.4 Binding assays

CHO-AQP4 cells or primary astrocytes were plated in 96-well microplates and grown for 18–24 h to confluence. Cells were washed twice with PBS and blocked with 1% bovine serum albumin (BSA) in live cell buffer (PBS containing 6 mM glucose, 1 mM sodium pyruvate) for 30 min. After removal of blocking solution, test antibody in 50 μl blocking buffer was added. After 1 h incubation at room temperature cells were washed three times with PBS over 5 min. In some experiments, cells were fixed in 2% paraformaldehyde (PFA) prior to washing. Then, washed cells were incubated with horseradish peroxidase (HRP)-labeled goat anti-human IgG secondary antibody (1:1000; Jackson ImmunoResearch) for 30

min at room temperature. After washing five times with PBS, HRP activity was assayed by addition of 50 μl Amplex red substrate (100 μM, Sigma) and 2 mM H_2O_2 as described (Phuan et al., 2013). Fluorescence was measured after 10 min (excitation/emission 540/590 nm) using an Infinite M1000 plate reader (Tecan Ltd, Mannedorf, Switzerland). To measure the time course of AQmab^{AM} binding and unbinding, CHO-AQP4 cells were incubated for different times (2, 5, 10, 15, 30, 60, 75 min) to determine binding kinetics, or incubated with AQmab^{AM} for 1h followed by washing and incubation for different times (0.5, 1, 2, 4, 6 h) to determine unbinding kinetics.

2.5 Complement-dependent cytotoxicity (CDC)

CHO-AQP4 cells were plated onto 96-well microplates at 25,000 cells/well and grown for 18–24 h to confluence. Cells were washed with PBS and incubated for 60 min with rAb-53 or various affinity-matured antibodies (without Fc mutations) together with 1–2% human complement in 50 μl live cell buffer at 27 °C or 37 °C. To measure cytotoxicity, cells were washed twice with PBS and incubated with 50 μl of a 20% Alamar blue solution (Invitrogen) for 45 min at 37 °C. Cytotoxicity was measured from resorufin fluorescence (excitation/emission 560/590 nm). Percentage cytotoxicity was calculated as: (negative control – compound) / (negative control – positive control) × 100. As negative control cells were treated with human complement only, and as positive control cells were treated with 0.1% Triton-X100.

2.6 Aquaporumab cytotoxicity protection assays

For assay of CDC, CHO-AQP4 cells were incubated for 1 h with AQmab^{AM}, then for 1 h at 37 °C with rAb-53 (0.2, 0.5, 1 μg/ml) or 1–2% heat-inactivated NMO patient sera and 2% human complement. In some experiments, AQmab^{AM} was added 1 h prior to, together with, or 1 h after addition of rAb-53. For assay of ADCC, CHO-AQP4 cells were incubated for 1 h with AQmab^{AM}, then for 1 h at 37 °C with 1–2% NMO patient sera and NK effector cells (effector : target ratio 20:1). Cytotoxicity were measured using the Alamar blue assay. In some studies, 1 μM calcein-AM and 2 μM ethidium-homodimer (Invitrogen) were added to stain live cells green and dead cells red for visualization by fluorescence microscopy.

2.7 Competitive binding assays

To measure binding of AQP4-IgG in NMO patient sera, AQmab^{AM} was treated with IdeS (IgG-degrading enzyme of S. *pyogenes*) to cleave its Fc sequence (to prevent its detection with anti-human secondary antibody). IdeS microspin columns (FragIT Microspin) were purchased from Genovis Inc. (Cambridge, MA) (Tradtrantip et al., 2013). AQmab^{AM} was treated by incubation for 1 h at 37 °C in the column (IdeS coupled to agarose beads) (1–5 units per μg IgG) and then eluted. The treated antibody is referred to as AQmab^{IdeS}. The efficacy of IdeS treatment was confirmed by staining with goat anti-human IgG, F(ab')$_2$ fragment (1:1000; Jackson ImmunoResearch) or Fc fragment-specific, HRP-conjugated secondary antibody (1:1000; Jackson ImmunoResearch). For competitive binding experiments, CHO-AQP4 cells were incubated with AQmab^{IdeS} for 1 h at room temperature, then human NMO sera were added for an additional 1 h. After fixation and washing, horseradish peroxidase (HRP)-labeled goat anti-human IgG, Fc fragment-specific secondary

antibody (1:1000; Jackson ImmunoResearch) was added to detect bound serum IgG antibodies.

2.8 Immunofluorescence

CHO-AQP4 cells or primary astrocytes were plated onto coverslips in 24-well plates and grown for 18–24 h to confluence. After blocking with 1% BSA in PBS, cells were incubated with AQmab^{IdeS} for 30 min at room temperature. Cells were washed with PBS and incubated with Cy3-conjugated AffiniPure goat anti-human IgG, F(ab)$_2$ fragment-specific, secondary antibody (1:200; Jackson ImmunoResearch), or Alexa Fluor-555 goat anti-human IgG, Fc fragment-specific, secondary antibody (1:500, Invitrogen). For AQP4 immunostaining, cells were fixed in 4% PFA and permeabilized with 0.1% Triton-X. Rabbit anti-AQP4 antibody (1:200, Santa Cruz) was added followed by Alexa Fluor-488 goat anti-rabbit IgG secondary antibody (1:500, Invitrogen).

3. Results

3.1 Binding of affinity-matured anti-AQP4 antibodies to AQP4

The antibodies studied herein were of the IgG1 isotype, some with Fc mutations L234A/L235A to neutralize CDC and ADCC effector functions (Tradtrantip et al., 2012b), and some containing mutations in their Fab region to increase their binding affinity to AQP4 (Figure 1A). Antibodies were assayed for their binding to the extracellular region of AQP4 in CHO cells stably expressing the M23 isoform of human AQP4, in which AQP4 tetramers cluster in supramolecular aggregates called ‘orthogonal arrays of particles’ (Smith et al., 2014), as found in native AQP4-expressing astrocytes. A cell-based ELISA was used in which binding of the human IgG antibody was detected using a HRP-conjugated anti-human secondary antibody and Amplex red substrate (Figure 1B).

Figure 1C shows representative binding curves of Amplex red fluorescence as a function of antibody concentration. Data are shown for the original aquaporumab based on the rAb-53 sequence (Tradtrantip et al., 2012b), as well as for several antibodies containing affinity-enhancing Fab mutations. Data are shown for antibodies with non-mutated Fc (WT) and with L234A/L235A effector function-neutralizing mutations (LL). Data fitted well to a single-site binding model. No significant binding was seen for an isotype-matched control antibody (2B4). The apparent AQP4 binding affinity (K_d) of the original rAb-53 aquaporumab was 145 ± 9 ng/ml (S.E.M., 4 sets of measurements). Figure 1D summarizes the fold-enhancements in AQP4 binding affinity of three antibodies with single point mutations obtained from the initial step of affinity maturation in which single point mutations in CDRs were tested individually, prior to generating and testing of mutation combinations. The affinity-matured antibody with greatest AQP4 binding affinity, which contained the two Fab mutations Y50R and S56R (referred to below as AQmab^{AM}), had ~8-fold improved AQP4 binding affinity (K_d 18 ng/ml, ~0.12 nM) compared to the original aquaporumab. The L234A/L235A Fc mutations had little effect on AQP4 binding for the various antibodies tested.

In a control study, binding curves were generated using the method in Figure 1B, except that a fixation step was included after antibody incubation and prior to washing to test whether the binding assay might be affected by antibody washout and antibody unbinding. Figure 1E shows similar affinities for studies done without vs. with the added fixation step for AQmab^{AM} (K_d 18 vs. 17 ng/ml, without vs. with fixation step). In separate studies, the rates of binding and unbinding of AQmab^{AM} to AQP4 were measured by varying antibody incubation and washout times (Figure 1F). The half-time ($t_{1/2}$) for AQmab^{AM} binding was ~15 min. Little AQmab^{AM} unbinding was seen at 1 h, with 50% unbinding at ~4 h. Antibody binding was also measured to native AQP4 in primary cultures of murine astrocytes, anticipating similar binding as in CHO cells expressing human AQP4. Figure 1G confirmed that antibody binding affinities were similar to those measured in Figure 1C using CHO-AQP4 cells. Figure 1H shows high magnification confocal imaging of antibody-stained CHO-AQP4 cells and astrocytes, detected using Alexa Fluor-555 goat anti-human IgG secondary antibody. The overlapping AQP4 and antibody expression showed a distinct punctate membrane pattern characteristic of AQP4 membrane clustering.

3.2 Complement-dependent cytotoxicity produced by affinity-matured anti-AQP4 antibodies

The greater AQP4 binding affinity of the affinity-matured antibodies found in binding assays in Figure 1 predict that the antibodies containing Fab (but not Fc) mutations would have a greater potency (EC_{50}) for cell killing. Complement-dependent cytotoxicity was measured in AQP4-expressing cells incubated with antibody and human complement, with Alamar blue readout of cell viability (Figure 2A). Figure 2B shows cell killing curves as percentage cytotoxicity as a function of antibody concentration. Antibody and complement incubations were done at both 27 °C and 37 °C to reveal possible temperature effect. Antibody concentration-dependent cytotoxicity was seen for the various antibodies tested, with improved killing potency for the affinity-matured antibodies compared with rAb-53. Antibodies containing Fc mutations L234A/L235A showed little killing (<10% cytotoxicity at 1000 mg/ml, data not shown). Figure 2C shows representative live-dead cell staining in which the affinity-matured antibody Y50R/S56R was incubated with human complement at 27 °C or 37 °C, showing substantially greater killing than that produced by rAb-53 at same concentration.

EC_{50} values for cell killing are summarized in Figure 2D. Compared to killing by rAb-53, EC_{50} values for killing by 50R/56R (AQmab^{AM}) and 30F/56R were ~6-fold and 3-fold lower, respectively. For comparison, K_d values for AQP4 binding (from data in Figure 1) are shown. Though comparable fold-improvements in EC_{50} for killing and K_d for AQP4 binding were seen with affinity-matured antibodies, ~4-fold greater antibody concentrations were needed for killing than for binding, which is in part the consequence of the multivalent interactions of antibody with the C1q component of complement (Phuan et al., 2012; Soltys et al., 2019).

3.3 Protection against AQP4-IgG-dependent complement-dependent cytotoxicity by affinity-matured aquaporumab

The important property of an aquaporumab blocking antibody for its use in NMO is its efficacy in protection against cytotoxicity caused by AQP4-IgG autoantibodies. To initially characterize the protection assay to be used with NMO patient sera, CDC was measured in AQP4-expressing CHO cells that were incubated with AQmab^{AM} followed by the recombinant monoclonal antibody rAb-53 (without Fc mutations) and human complement, with Alamar blue readout of cytotoxicity (Figure 3A, left). Cytotoxicity protection curves shown in Figure 3A (right) were generated using 3 concentrations of rAb-53, each producing different percentages cytotoxicity (in the absence of AQmab^{AM}). In each case AQmab^{AM} concentration-dependent protection against CDC was seen, with complete protection at high AQmab^{AM} concentrations. The apparent IC_{50} values for protection depended on rAb-53 concentration, as expected for a competitive mechanism.

Order of addition studies were done in which AQmab^{AM} was added 1 h before, together with, or 1 h after rAb-53 and human complement. Cell killing was measured using the Alamar blue assay. Figure 3B shows that AQmab^{AM} incubated prior to rAb-53 afforded the best protection. Addition of AQmab^{AM} at the same time as rAb-53 gave incomplete protection even at high concentration, and AQmab^{AM} added after rAb-53 showed little protection, which is not unexpected because of the slow kinetics of antibody unbinding from AQP4.

Figure 3C compares the protection efficacy of the original (rAb-53-based) vs. the affinity-matured aquaporumab. The apparent IC_{50} for cytoprotection was ~8-fold greater for AQmab^{AM} than for the rAb-53-based aquaporumab, similar to the fold increase in AQP4 binding found in Figure 1.

AQmab^{AM} protection against CDC was next studied in serum samples obtained from confirmed AQP4-IgG seropositive NMO patients. All sera were heat-treated to inactivate any endogenous active complement. (The heat treatment did not affect antibody binding to AQP4, not shown). CDC curves for each human serum specimen were initially generated to determine appropriate dilutions of serum to use that produced ~40–60% cytotoxicity, with examples shown in Figure 4A. Little cytotoxicity was seen with control (non-NMO) sera.

For CDC protection studies, AQP4-expressing CHO cells were first incubated with AQmab^{AM}, followed by addition of (heat-inactivated) human NMO serum and human complement, with Alamar blue readout of cytotoxicity (Figure 4B). Figure 4C shows CDC protection curves with cytotoxicity plotted as a function of aquaporumab concentration for studies done using sera from four NMO patients, each studied in parallel with a non-NMO control serum. Antibody concentration-dependent protection against cytotoxicity was seen, with near-complete protection at high antibody concentrations. Figure 4D summarizes IC_{50} values for half-protection against CDC for eight NMO patient sera. IC_{50} values for AQmab^{AM} ranged from 40–80 ng/ml, which were ~8-fold lower than for the original rAb-53-based aquaporumab. Figure 4E shows examples of live-dead cell staining in which live cells are stained green and dead cells red. Incubation of cells with NMO patient serum

and human complement produced marked cell death, which was reduced to a much greater extent by preincubation with AQmab^{AM} than the original rAb-53-based aquaporumab.

3.4 Protection against AQP4-IgG antibody-dependent cellular cytotoxicity by affinity-matured aquaporumab

Antibody protection studies were also done for killing of CHO-AQP4 cells by an ADCC mechanism in which CHO-AQP4 cells were incubated with AQmab^{AM} (or original rAb-53-based aquaporumab) followed by addition of NMO sera and NK cells (in the absence of complement), with Alamar blue readout of cytotoxicity (Figure 5A). Figure 5B shows ADCC protection curves for the same four NMO patient sera as tested in the CDC protection assays in Figure 4C. Aquaporumab concentration-dependent protection against ADCC was seen, with complete protection at high concentrations. Little cytotoxicity was seen with control (non-NMO) sera. Figure 5C summarizes IC_{50} values for protection against ADCC, which ranged from 30–80 ng/ml for AQmab^{AM}, ~7-fold lower than for the original rAb-53-based aquaporumab. Figure 5D shows examples of live-dead cell staining, with marked cell death produced by the NMO serum and NK cells. Much less cell death was seen with AQmab^{AM} than with the original aquaporumab.

3.5 AQmab^{AM} competes with AQP4-IgG in NMO patient sera for AQP4 binding

The presumed mechanism of AQmab^{AM} protection against CDC and ADCC caused by NMO patient sera is competition between AQmab^{AM} and patient serum AQP4-IgG for binding to AQP4. To test this mechanism, AQmab^{AM} was first treated with the enzyme IdeS in order to cleave its Fc portion in the lower hinge region, leaving F(ab')$_2$ (Figure 6A), to enable detection of AQP4-IgG in NMO sera using a Fc-specific secondary antibody. The original and IdeS-cleaved AQmab^{AM} (called AQmab^{IdeS}) bound identically to AQP4 on CHO-AQP4 cells, as detected using a HRP-conjugated F(ab')$_2$-specific secondary antibody, with little signal seen with a Fc-specific antibody (Figure 6B, left), demonstrating efficient cleavage. This was verified by immunofluorescence in Figure 6B (right), which shows AQP4 immunofluorescence (green) on CHO-AQP4 cells, co-stained with AQmab^{IdeS} detected using a Cy3-conjugated F(ab')$_2$-specific secondary antibody or an AF-555 conjugated Fc-specific secondary antibody (red).

Figure 6C shows the competition binding assay in which AQP4-expressing CHO cells were treated with AQmab^{IdeS} followed by NMO patient serum, in which bound AQP4-IgG in NMO serum was revealed using a Fc-specific secondary antibody with HRP / Amplex red readout. Binding competition curves for sera from two NMO patients show AQmab^{IdeS} concentration-dependent competition for binding, with half-competition at ~60 ng/ml AQmab^{IdeS}, similar to IC_{50} values for protection against CDC and ADCC by AQmab^{AM}.

4. Discussion

AQP4-IgG seropositive neuromyelitis optica spectrum disorder is an autoimmune disease that is uniquely suited to antibody blocking therapy because it is caused by circulating autoantibodies that initiate cellular pathology by binding to a small, well-defined, cell-surface exposed target, AQP4. Other autoimmune disorders, such as systemic lupus

erythematosus, Sjögren's syndrome and type I diabetes, do not have a validated single, small target and/or have uncertain pathogenesis mechanisms (Ludwig et al., 2017). Some disorders, such as Graves' disease, Myasthenia gravis, and thrombotic thrombocytopenic purpura, may be amenable to antibody blocking therapy though to our knowledge an antibody blocking approach has not been advanced or tested for any autoimmune disease.

Effective anti-AQP4 antibody blocking therapy in NMO requires that the antibody therapeutic possess sufficiently high affinity and be present at sufficiently high concentration to block, by competition, binding of pathogenic AQP4-IgG. The original aquaporumab was based on the fully human NMO monoclonal antibody rAb-53, which was found to have the highest affinity of >30 AQP4-binding antibodies tested, as well as very slow unbinding kinetics compared to other antibody candidates (Crane et al., 2011; Tradtrantip et al., 2012b). Affinity maturation here generated an antibody, AQmab^{AM}, with ~8-fold greater binding affinity to AQP4 than the original aquaporumab, which blocked cytotoxicity, by both CDC and ADCC mechanisms, produced by multiple NMO patient sera with IC_{50} for cytoprotection in a remarkably narrow range of 30–80 ng/ml. The aquaporumab K_d for AQP4 binding and the IC_{50} for cytoprotection that are sufficient to confer clinical benefit in human NMO are difficult to estimate, as they depend on aquaporumab accumulation in CNS tissues at sites of active NMO pathology in which blood-CNS barrier integrity is impaired, as well as on the properties and concentrations of the complex and shifting polyclonal AQP4-IgG antibody mixture present in NMO patient sera. For reference, typical maximum concentrations (C_{max}) of therapeutic monoclonal antibodies, as used for example for treatment of Non-Hodgkin's lymphoma and rheumatoid arthritis, are in the range 60–500 mg/L (60,000–500,000 ng/ml) (Leveque et al, 2005, Keizer et al, 2010), substantially greater than the IC_{50} of 40–80 ng/ml of the affinity-matured aquaporumab measured herein, even after multiplication by a factor of up to 100 to account for serum dilution (giving 4,000–8,000 ng/ml). Additional multiplication by a factor of 5 (giving 20,000–40,000 ng/ml) predicts > 90% protection against cytotoxicity at attainable serum antibody concentrations. We note that experimental animal studies are unlikely to be informative on aquaporumab properties for efficacy in human NMO because available animal models, such as those produced by intracranial or intravenous administration of AQP4-IgG, require additional effectors of neuroinflammation such as brain injury, T cell activation or administration, or various pro-inflammatory maneuvers (Bradl and Lassman, 2014; Li and Yan, 2015; Duan and Verkman, 2019). Available experimental animal models of NMO are limited and no model to date closely recapitulates spontaneous anti-AQP4 autoimmunity with the clinical and pathological features of human NMO.

If safe and effective, aquaporumab therapy may be suitable for use as monotherapy of NMO, both to treat and prevent disease exacerbations, or in combination with one or more currently used drugs such as immunosuppressants. The potential advantages of aquaporumab therapy over currently used (off-label) therapies, or the newer biologics targeting complement C5, IL-6 receptors or CD19, which may soon be approved for NMO, is that aquaporumab is highly targeted and does not have immunosuppressive actions that can increase risks for malignancy and infections. Aquaporumab antibody therapy is unlikely to have significant toxicity based on the observation that NMO patients can have circulating AQP4-IgG autoantibodies for many years without clinical disease (Jarius and Wildemann, 2010; Jarius

et al., 2014), and, except for a few case reports of NMO-related myositis (Guo et al., 2014; Malik et al., 2014), peripheral disease in AQP4-expressing tissues such as kidney, lung and stomach has not been seen. We note, however, that some cell culture studies report actions of AQP4-IgG on cytokine release that are independent of complement and cellular cytotoxicity mechanisms (Haruki et al., 2013; Howe et al., 2014), as well as AQP4-IgG cellular internalization (Hinson et al., 2012), though we have not seen AQP4-IgG internalization to toxicity in polarized astrocytes in vivo (Ratelade et al., 2011; Rossi et al., 2012).

In conclusion, our study advances the development of an aquaporumab blocking antibody strategy for potential therapy of AQP4-IgG seropositive neuromyelitis optica spectrum disorder. The affinity-matured antibody, by a presumably steric competitive mechanism, blocks binding and cytotoxicity of polyclonal AQP4-IgG in NMO patient sera in vitro, which is predicted to translate to clinical benefit in human NMO. Further development of aquaporumab for NMO therapy will require characterization and optimization of antibody pharmacokinetics and other pharmacological properties, as well as evaluation of potential toxicity following long-term administration.

Acknowledgments

This work was supported by grants from the Guthy-Jackson Charitable Foundation (to ASV and JLB), grants EY13574, DK72517 and DK101373 (to ASV) and EY022936 (to JLB) from the National Institutes of Health, a grant from the Focused Ultrasound Foundation (to ASV). We thank Kimberly Clawson-Stone and Peyton Henderson for recombinant antibody production.

Abbeviations:

ADCC	antibody-dependent cellular cytotoxicity
AQmab^{AM}	affinity-matured aquaporumab
AQmab^{IdeS}	IdeS-cleaved AQmab^{AM}
AQP4	aquaporin-4
AQP4-IgG	aquaporin-4 immunoglobulin G
BSA	bovine serum albumin
CDC	complement-dependent cytotoxicity
CDR	complementary determining region
CHO	Chinese hamster ovary
EC_{50}	half-maximal effective concentration
Fab	antigen-binding fragment
$F(ab)_2$	two antigen-binding fragment portions
Fc	the fragment crystallizable region
HRP	horseradish peroxidase

IC_{50}	half-maximal inhibitory concentration
IdeS	IgG-degrading enzyme of *Streptococcus pyogenes*
K_d	binding constant
NMO	neuromyelitis optica
NMOSD	neuromyelitis optica spectrum disorders
PBS	phosphate-buffered saline
PFA	paraformaldehyde
$t_{1/2}$	half time
2B4	isotype-matched antibody control

References

Bennett JL, Lam C, Kalluri SR, Saikali P, Bautista K, Dupree C, Glogowska M, Case D, Antel JP, Owens GP, Gilden D, Nessler S, Stadelmann C, Hemmer B, 2009 Intrathecal pathogenic anti-aquaporin-4 antibodies in early neuromyelitis optica. Ann Neurol 66, 617–629. [PubMed: 19938104]

Bradl M, Lassmann H 2014 Experimental models of neuromyelitis optica. Brain Pathol 24, 74–82. [PubMed: 24345221]

Bruscolini A, Sacchetti M, La Cava M, Gharbiya M, Ralli M, Lambiase A, De Virgilio A, Greco A Diagnosis and management of neuromyelitis optica spectrum disorders – an update. Autoimmun Rev 17, 195–200. [PubMed: 29339316]

Collongues N, Ayme-Dietrich E, Monassier L, de Seze J 2919 Pharmacotherapy for neuromyelitis optica spectrum disorders: current management and future options. Drugs 79, 125–142.

Crane JM, Lam C, Rossi A, Gupta T, Bennett JL, Verkman AS, 2011 Binding affinity and specificity of neuromyelitis optica autoantibodies to aquaporin-4 M1/M23 isoforms and orthogonal arrays. J Biol Chem 286, 16516–16524. [PubMed: 21454592]

Duan T, Smith AJ, Verkman AS, 2018 Complement-dependent bystander injury to neurons in AQP4-IgG seropositive neuromyelitis optica. J Neuroinflammation 15, 294. [PubMed: 30348195]

Duan T, Verkman AS 2019 Experimental animal models of aquaporin-4-IgG seropositive neuromyelitis spectrum disorders: progress and shortcomings. Brain Pathol. In press.

Graber DJ, Levy M, Kerr D, Wade WF, 2008 Neuromyelitis optica pathogenesis and aquaporin 4. J Neuroinflammation 5, 22. [PubMed: 18510734]

Guo Y, Lennon VA, Popescu BF, Grouse CK, Topel J, Milone M, Lassmann H, Parisi JE, Pittock SJ, Stefoski D, Balabanov R, Lucchinetti CF 2014 Autoimmune aquaporin-4 myopathy in neuromyelitis optica spectrum. JAMA Neurol 71, 1025–1029. [PubMed: 24911400]

Haruki H, Sano Y, Shimizu F, Omoto M, Tasaki A, Oishi M, Koga M, Saito K, Takahashi T, Nakada T, Kanda T 2013 NMO sera down-regulate AQP4 in human astrocyte and induce cytotoxicity independent of complement. J Neurol Sci 331, 136–144. [PubMed: 23809190]

Hinson SR, Romero MF, Popescu BF, Lucchinetti CF, Fryer JP, Wolburg H, Fallier-Becker P, Noell S, Lennon VA 2012 Molecule outcomes of neuromyelitis optic (NMO)-IgG binding to aquaporin-4 in astrocytes. Proc Natl Acad Sci USA 109, 1245–1250. [PubMed: 22128336]

Howe CL, Kaptzan T, Magaña SM, Ayers-Ringler JR, LaFrance-Corey RG, Lucchinetti CF 2014 Neuromyelitis optica IgG stimulates an immunological response in rat astrocyte cultures. Glia 62, 692–708. [PubMed: 24492996]

Jarius S, Wildemann B 2010 AQP4 antibodies in neuromyelitis optica: diagnostic and pathogenetic relevance. Nat Rev Neurol 6, 383–392. [PubMed: 20639914]

Jarius S, Wildemann B, Paul F 2014 Neuromyelitis optica: clinical features, immunopathogenesis and treatment. Clin Exp Immunol 176, 149–164. [PubMed: 24666204]

Keizer RS, Huitema AD, Schellens JH, Beijnen JH, 2010 Clinical pharmacokinetics of therapeutic monoclonal antibodies. Clin Pharmacokinet 49, 493–507. [PubMed: 20608753]

Lennon VA, Kryzer TJ, Pittock SJ, Verkman AS, Hinson SR, 2005 IgG marker of optic-spinal multiple sclerosis binds to the aquaporin-4 water channel. J Exp Med 202, 473–477. [PubMed: 16087714]

Leveque D, Wisniewski S, Jehl L 2005 Pharmacokinetics of therapeutic monoclonal antibodies used in oncology. Anticancer Res 25, 2327–2344. [PubMed: 16080460]

Li M, Yan Y 2015 Experimental models of neuromyelitis optica: current status, challenges and future directions. Neurosci Bull 31, 735–744. [PubMed: 26109280]

Lucchinetti CF, Mandler RN, McGavern D, Bruck W, Gleich G, Ransohoff RM, Trebst C, Weinshenker B, Wingerchuk D, Parisi JE, Lassmann H, 2002 A role for humoral mechanisms in the pathogenesis of Devic's neuromyelitis optica. Brain 125, 1450–1461. [PubMed: 12076996]

Ludwig RJ, Vanhoorelbeke K, Leypoldt F, Kaya Z, Bieber K, McLachlan SM, Komorowski L, Luo J, Cabral-Marques O, Hammers CM, Lindstrom JM, Lamprecht P, Fischer A, Riemekasten G, Tersteeg C, Sondermann P, Rapoport B, Wandinger KP, Probst C, El Beidaq A, Schmidt E, Verkman AS, Manz RA, Nimmerjahn F, 2017 Mechanisms of autoantibody-induced pathology. Front Immunol 8, 603. [PubMed: 28620373]

Mader S, Brimberg L 2019 Aquaporin-4 water chanel in the brain and its implication for health and disease. Cells 8(2).

Malik R, Lewis A, Cree BA, Ratelade J, Rossi A, Verkman AS, Bollen AW, Ral;h JW 2014 Transient hyperCKemia in the setting of neuromyelitis optica. Muscle Nerve 50, 859–862. [PubMed: 24862586]

Misu T, Fujihara K, Kakita A, Konno H, Nakamura M, Watanabe S, Takahashi T, Nakashima I, Takahashi H, Itoyama Y, 2007 Loss of aquaporin 4 in lesions of neuromyelitis optica: distinction from multiple sclerosis. Brain 130, 1224–1234. [PubMed: 17405762]

Papadopoulos MC, Bennett JL, Verkman AS, 2014 Treatment of neuromyelitis optica: state-of-the-art and emerging therapies. Nat Rev Neurol 10, 493–506. [PubMed: 25112508]

Papadopoulos MC, Verkman AS, 2012 Aquaporin 4 and neuromyelitis optica. Lancet Neurol 11, 535–544. [PubMed: 22608667]

Phuan PW, Ratelade J, Rossi A, Tradtrantip L, Verkman AS, 2012 Complement-dependent cytotoxicity in neuromyelitis optica requires aquaporin-4 protein assembly in orthogonal arrays. J Biol Chem 287, 13829–13839. [PubMed: 22393049]

Phuan PW, Zhang H, Asavapanumas N, Leviten M, Rosenthal A, Tradtrantip L, Verkman AS, 2013 C1q-targeted monoclonal antibody prevents complement-dependent cytotoxicity and neuropathology in in vitro and mouse models of neuromyelitis optica. Acta Neuropathol 125, 829–840. [PubMed: 23677375]

Ratelade J, Bennett JL, Verkman AS, 2011 Evidence against cellular internalization in vivo of NMO-IgG, aquaporin-4, and excitatory amino acid transporter 2 in neuromyelitis optica. J Biol Chem 286, 45156–45164. [PubMed: 22069320]

Rossi A, Ratelade J, Papadopoulos MC, Bennett JL, Verkman AS, 2012 Neuromyelitis optica IgG does not alter aquaporin-4 water permeability, plasma membrane M1/M23 isoform content, or supramolecular assembly. Glia 60, 2027–2039. [PubMed: 22987455]

Smith AJ, Jin BJ, Ratelade J, Verkman AS 2014 Aggregation state determines the localization and function of M1- and M23-Aquaporin-4 in astrocytes. J Cell Biol 204, 559–573. [PubMed: 24515349]

Soltys J, Liu Y, Ritchie A, Wemlinger S, Schaller K, Schumann H, Owens GP, Bennett JL, 2019 Membrane assembly of aquaporin-4 autoantibodies regulates classical complement activation in neuromyelitis optica. J Clin Invest 130, 383–396.

Tradtrantip L, Asavapanumas N, Verkman AS, 2013 Therapeutic cleavage of anti-aquaporin-4 autoantibody in neuromyelitis optica by an IgG-selective proteinase. Mol Pharmacol 83, 1268–1275. [PubMed: 23571414]

Tradtrantip L, Yao X, Su T, Smith AJ, Verkman AS 2017 Bystander mechanism for complement-initiated early oligodendrocyte injury in neuromyelitis optica. Acta Neuropathol 134, 35–44. [PubMed: 28567523]

Tradtrantip L, Zhang H, Anderson MO, Saadoun S, Phuan PW, Papadopoulos MC, Bennett JL, Verkman AS, 2012a Small-molecule inhibitors of NMO-IgG binding to aquaporin-4 reduce astrocyte cytotoxicity in neuromyelitis optica. FASEB J 26, 2197–2208. [PubMed: 22319008]

Tradtrantip L, Zhang H, Saadoun S, Phuan PW, Lam C, Papadopoulos MC, Bennett JL, Verkman AS, 2012b Anti-aquaporin-4 monoclonal antibody blocker therapy for neuromyelitis optica. Ann Neurol 71, 314–322. [PubMed: 22271321]

Verkman AS, Phuan PW, Asavapanumas N, Tradtrantip L, 2013 Biology of AQP4 and anti-AQP4 antibody: therapeutic implications for NMO. Brain Pathol 23, 684–695. [PubMed: 24118484]

Weinshenker BG, Wingerchuk DM 2017 Neuromyelitis spectrum disorders. Mayo Clin Proc. 92, 663–679. [PubMed: 28385199]

Highlights

- Neuromyelitis optica spectrum disorder (NMOSD) is an autoimmune inflammatory disease of the central nervous system
- Seropositive NMOSD is caused by binding of pathogenic IgG autoantibodies to water channel aquaporin-4 on astrocytes
- Aquaporumab is an engineered human monoclonal IgG antibody, with effector functions neutralized, that strongly binds to aquaporin-4
- An affinity matured aquaporumab blocked NMOSD autoantibody binding to aquaporin-4 and prevented complement and cellular cytotoxicity

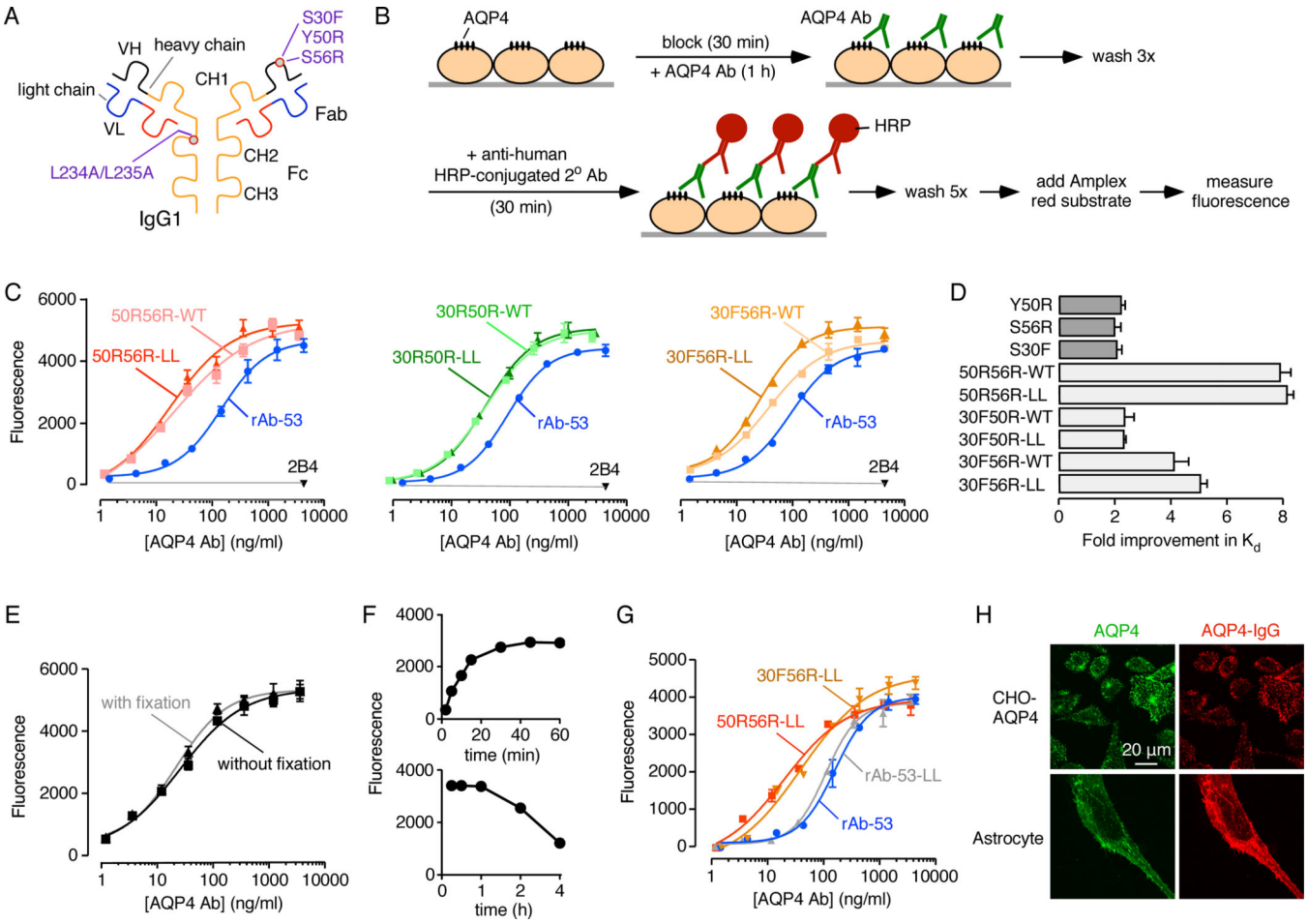

Figure 1.

Binding affinity of aquaporumab antibodies to CHO-AQP4 cells and primary astrocyte cultures. A. Structure of aquaporumab showing Fc mutations L234A/L235A and Fab mutations S30F, Y50R and S56R. VH, heavy chain; VL, light chain; CH1, constant region 1 in heavy chain. B. Assay for measurement of AQP4-IgG binding to AQP4 on CHO-AQP4 cells. After 30 min blocking, cells were incubated with AQP4-IgG at room temperature for 1 h, followed by 30 min incubation with HRP-conjugated anti-human secondary antibody, with Amplex Red substrate added to read out HRP activity. C. Binding curves (Amplex red fluorescence vs. antibody concentration [AQP4 Ab]) for indicated antibodies, without (WT) or with (LL) Fc LL mutations, comparing with reference antibody rAb-53 (mean ± S.E.M., n=4) and control (isotype-matched) antibody 2B4. D. Fold-improvement in AQP4 binding K_d of antibodies with indicated single and double Fc mutations, compared with K_d for rAb-53 (mean ± S.E.M., n=4). E. Binding curves of affinity-matured antibody (50R56R-LL) as in C, comparing without vs. with 2% PFA fixation for 5 min prior to washing. F. Time course of binding and unbinding of 50R56R-LL. G. Binding assay as in C, but with primary rat astrocyte cultures (mean ± S.E.M., n=4). H. High-magnification confocal micrographs of AQP4 (green) and AQP4-IgG (red) immunofluorescence on CHO-AQP4 cells and astrocytes.

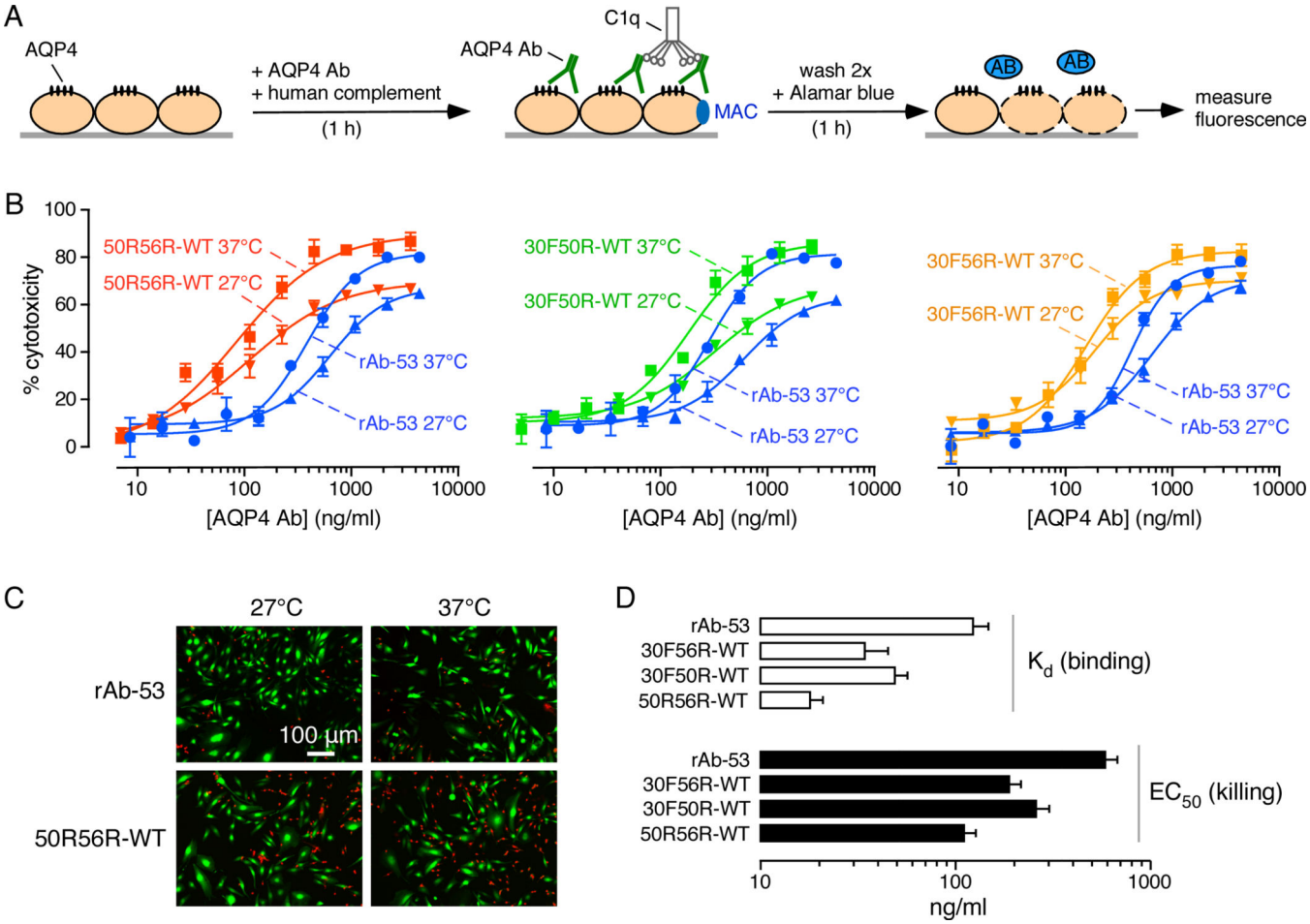

Figure 2.

Complement-dependent cytotoxicity in CHO-AQP4 cells produced by aquaporumab antibodies. A. Cytotoxicity was assayed 1 h incubation of cells with antibody and 2% human complement, following by readout of cytotoxicity using Alamar blue. B. Percentage cytotoxicity as a function of antibody concentration [AQP4 Ab], with antibody and complement incubations done at 27 or 37 °C (mean ± S.E.M., n=4). C. Live/dead cell imaging for experiments done as in B, with 200 ng/ml rAb-53 or affinity-matured antibody (without Fc mutations). D. EC_{50} values for killing, comparing with K_d for binding (from Fig. 1C) (mean ± S.E.M., n=4).

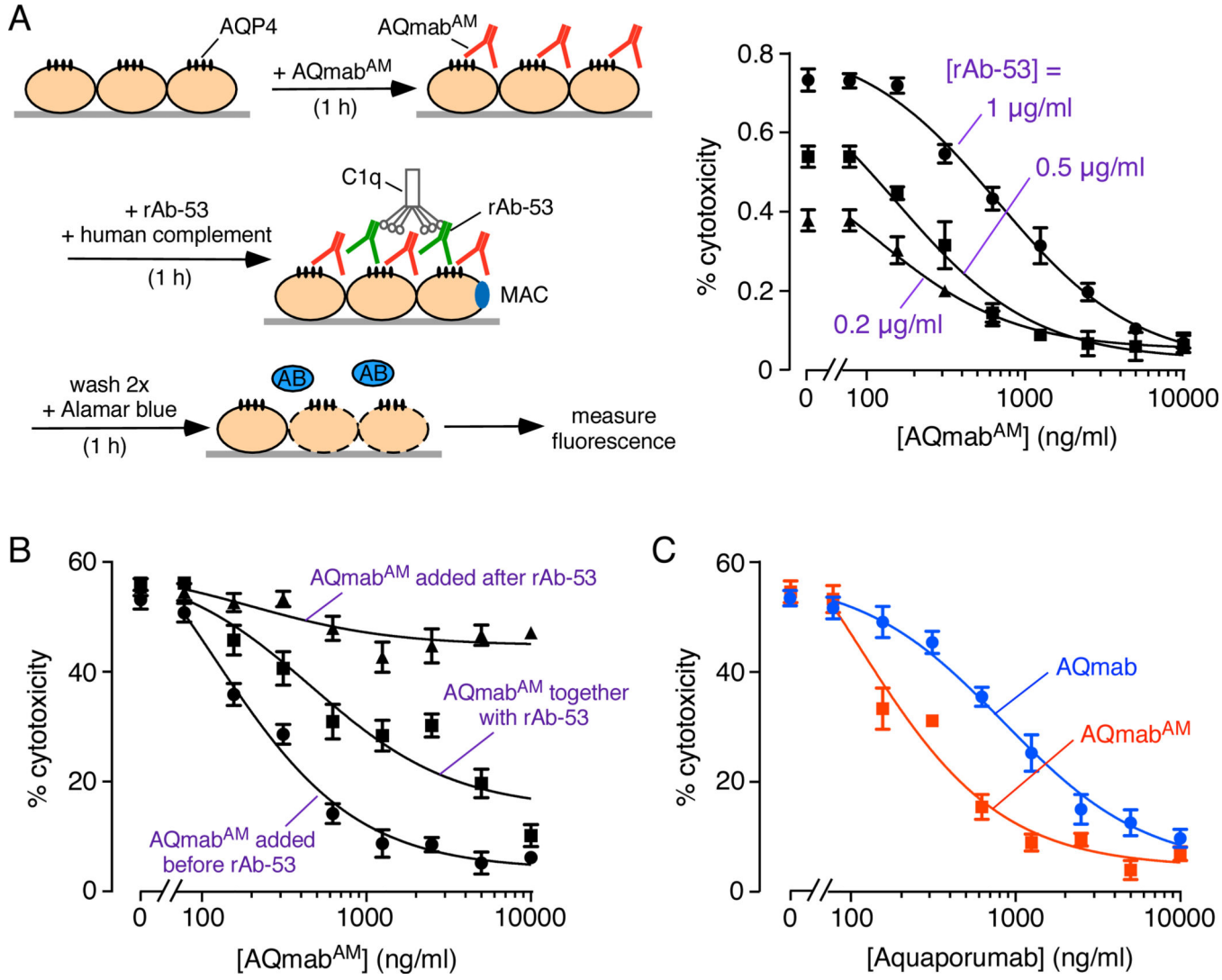

Figure 3.

AQmab^{AM} protection against complement-dependent cytotoxicity produced by rAb-53 and human complement. A. (Left) CHO-AQP4 cells were pre-incubated with AQmab^{AM} for 1 h, followed by addition of rAb-53 and human complement for 1 h. Cytotoxicity was assayed using Alamar blue. (Right) Percentage cytotoxicity as a function of AQmab^{AM} concentration for measurements done at different rAb-53 concentrations (mean ± S.E.M., n=3). B. Comparison of cytotoxicity with AQmab^{AM} added 1 h before, together with, or 1 h after rAb-53, followed by 2% human complement for an additional hour. Percentage cytotoxicity as a function of AQmab^{AM} concentration (mean ± S.E.M., n=3). C. Percentage cytotoxicity as in A, comparing protection by the original rAb-53-based aquaporumab (AQmab) and AQmab^{AM}.

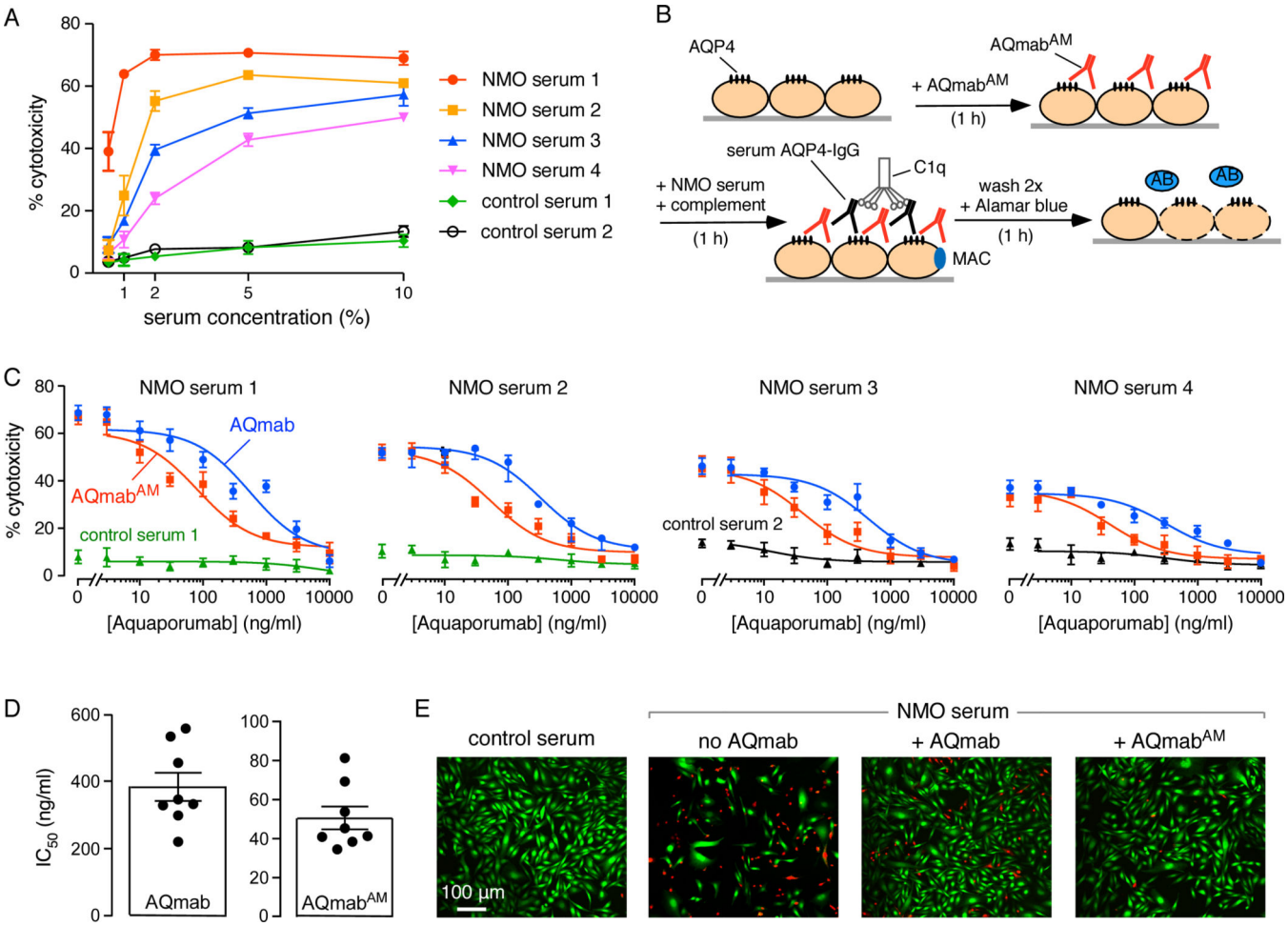

Figure 4.

AQmab^{AM} protection against complement-dependent cytotoxicity (CDC) produced by NMO patient sera and human complement. A. Cytotoxicity induced by 1 h incubation of heat-inactivated NMO sera and 2% human complement shown for sera from four NMO patients and two controls (mean ± S.E.M., n= 3). B. CHO-AQP4 cells were pre-incubated with AQmab^{AM} for 1 h, followed by addition of 1–2% serum and 2% human complement for 1 h. Cytotoxicity was assayed using Alamar blue. C. Cells were treated with 1–2% NMO serum from each of four different patients (or control serum) together with 2% human complement. Protection against cytotoxicity by original rAb-53-based aquaporumab (AQmab) compared with AQmab^{AM} (mean ± S.E.M., n=4). D. IC_{50} for protection against CDC by AQmab and AQmab^{AM} with each point representing a different NMO human serum (mean ± S.E.M., n=8). E. Live/dead cell assay as done in B with live cells stained green and dead cells stained red.

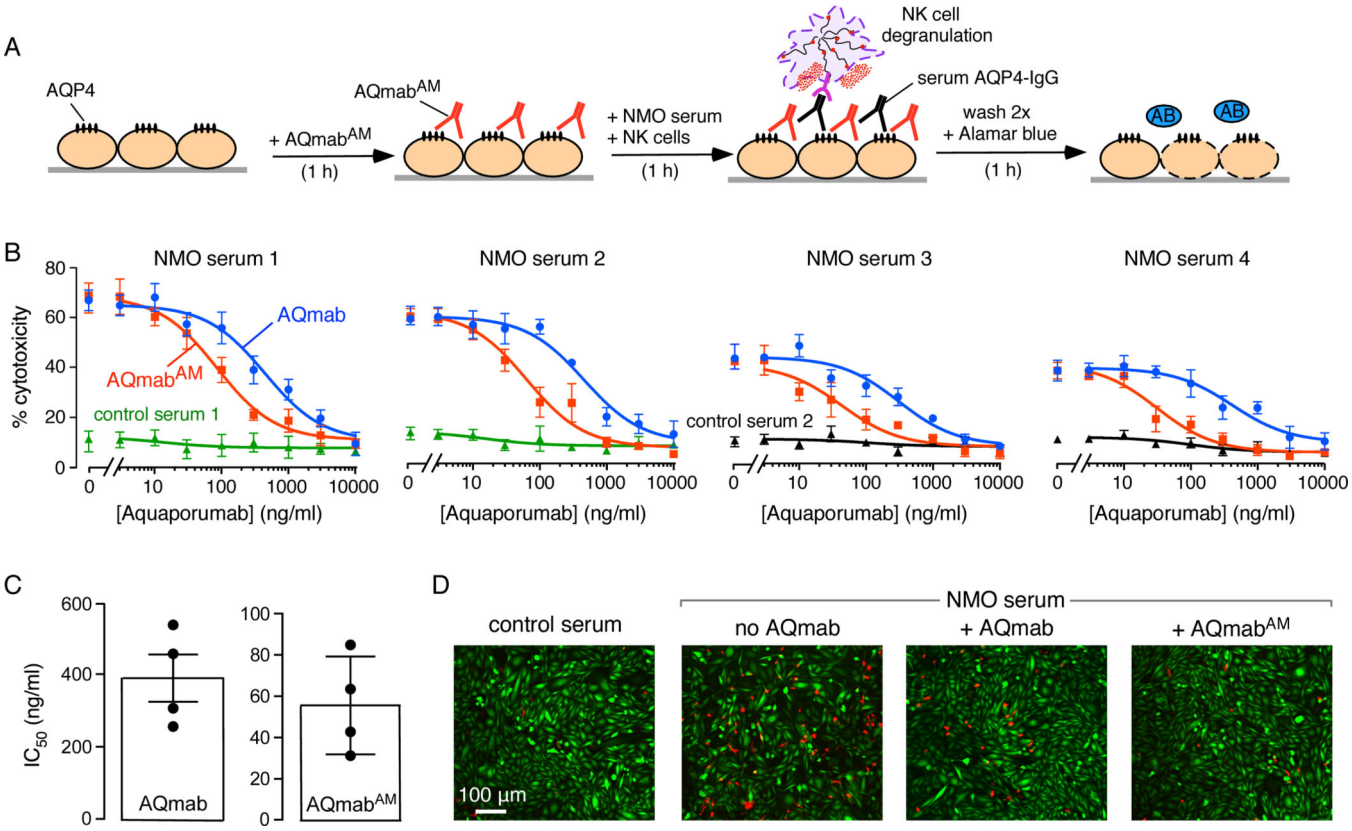

Figure 5.

AQmab^{AM} protection against antibody-dependent cellular cytotoxicity (ADCC) produced by NMO patient sera and NK cells. A. ADCC induced by 1 h incubation of 1–2% NMO serum and NK cells as effector cells, with AQmab^{AM} added prior to serum and NK cells. Cytotoxicity was measured using Alamar blue. B. AQmab^{AM} concentration-dependent protection against cytotoxicity as in A (mean ± S.E.M., n=4) using NMO sera four different patients. C. IC_{50} for protection against ADCC by AQmab and AQmab^{AM} with each point representing a different human NMO serum (mean ± S.E.M., n=4). D. Live/dead cell assay as done in B, with live cells stained green and dead cells stained red.

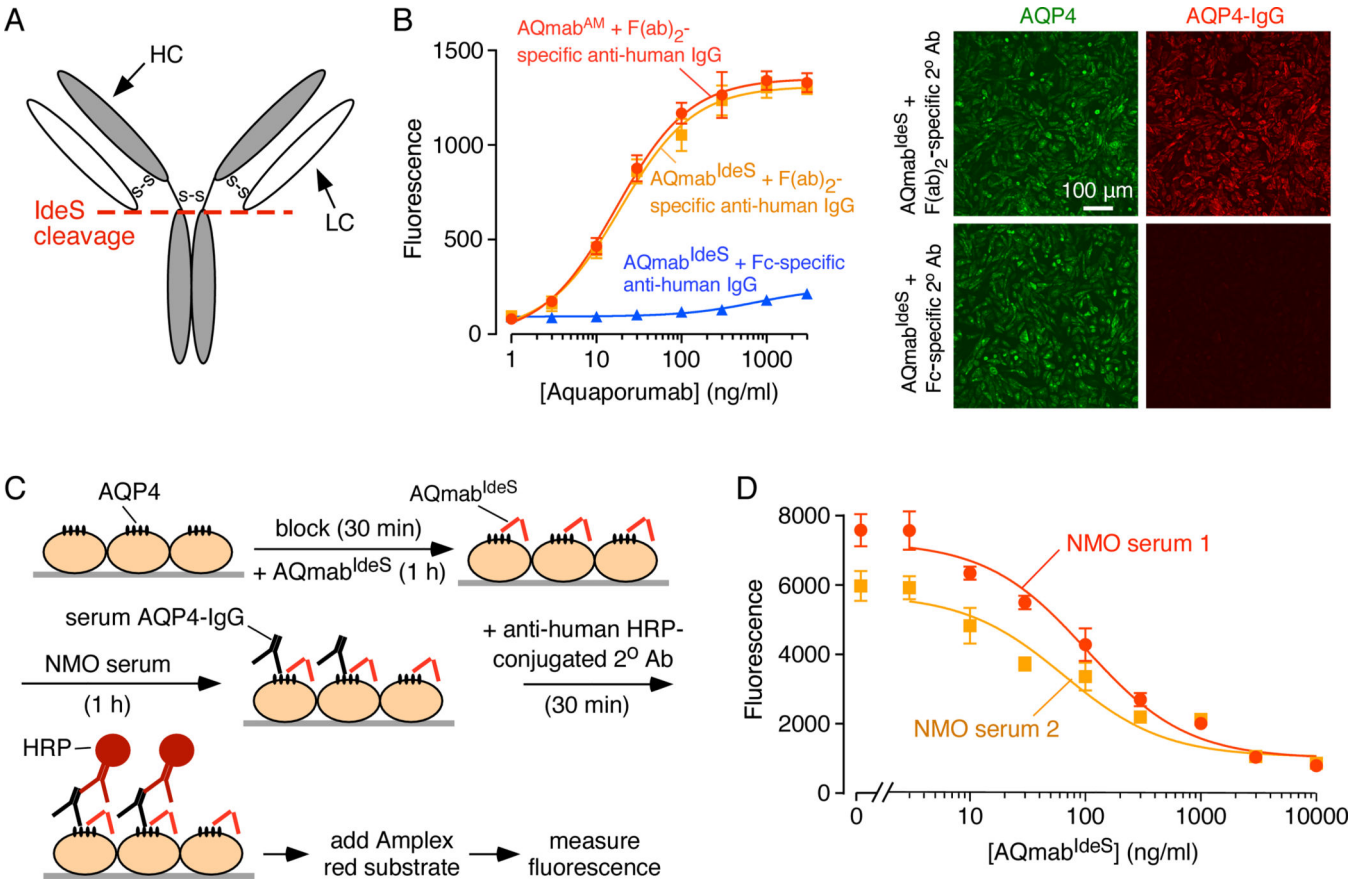

Figure 6.

AQmab^{AM} competes with AQP4-IgG in NMO patient sera for binding to AQP4 on CHO-AQP4 cells. A. Schematic showing IdeS cleavage of IgG at its lower hinge region, producing F(ab')$_2$ and Fc fragments. B. (Left) Binding of AQmab^{AM} (with or without IdeS treatment) to CHO-AQP4 cells. Fluorescence were detected by HRP-conjugated anti-human IgG, F(ab')$_2$ -specific, or Fc-specific, secondary antibody (mean ± S.E.M., n=3). (Right) Immunofluorescence showing binding of IdeS-cleaved AQmab^{AM} (AQmab^{IdeS}) to CHO-AQP4 cells using Cy3-conjugated goat anti-human IgG F(ab')$_2$ -specific, or Alexa 555-conjugated goat anti-human IgG Fc -specific secondary antibody. C. CHO-AQP4 cells were pre-incubated with AQmab^{IdeS} for 1 h then incubated with NMO serum for 1 h, followed by HRP-conjugated anti-human IgG Fc-specific secondary antibody to detect serum AQP4-IgG binding. D. AQmab^{IdeS} concentration-dependent displacement of AQP4-IgG in 1% NMO patient sera (mean ± S.E.M., n=3).